Journal of Cerebral Blood Flow & Metabolism (2014), e1–e9

www.jcbfm.com

NEGATIVE RESULT

The impact of Ly6C^{low} monocytes after cerebral hypoxia-ischemia in adult mice

Jean-Philippe Michaud[1,2], Pedro Moreno Pimentel-Coelho[1,2], Yannick Tremblay[1] and Serge Rivest[1]

After an ischemic stroke, mononuclear phagocytic cells such as microglia, macrophages, and monocytes migrate to the lesion site and coordinate an immune response. Monocytes, which are recruited from the bloodstream after ischemic brain injury, can be categorized into two subsets in mice: inflammatory and patrolling monocytes. Although inflammatory monocytes (Ly6C^{hi}) seem to have a protective role in stroke progression, the impact of patrolling monocytes (Ly6C^{low}) is unknown. To address the role of Ly6C^{low} monocytes in stroke, we generated bone marrow chimeric mice in which their hematopoietic system was replaced by *Nr4a1*$^{-/-}$ cells, allowing the complete and permanent ablation of Ly6C^{low} monocytes without affecting the Ly6C^{hi} subset. We then subjected adult mice to cerebral hypoxia-ischemia using the Levine/Vannucci model. Functional outcomes after stroke such as body weight change, neurologic score, motor functions and spatial learning were not affected. Moreover, depletion in Ly6C^{low} monocytes did not change significantly the total infarct size, cell loss, atrophy, the number, or the activation state of microglia/macrophages at the lesion site. These data suggest that Ly6C^{low} patrolling monocytes are redundant in the progression and recovery of ischemic stroke.

Journal of Cerebral Blood Flow & Metabolism (2014) **34**; doi:10.1038/jcbfm.2014.80; published online 30 April 2014

Keywords: blood; bone marrow transplantation; innate immunity; ischemia; Ly6C^{low} monocytes; stroke

INTRODUCTION

Despite the recent advances in understanding the complex cellular and molecular cascade of events triggered by cerebral ischemia, stroke remains as the third most common cause of long-term disability and the second leading cause of death worldwide.[1]

Cerebral ischemia is followed by the trafficking of inflammatory cells into the brain, as demonstrated by the presence of 'inflammatory infiltrates' in human brain samples and by several studies using animal models of stroke.[2] Indeed, although recent reports have revealed the embryonic origin of resident microglia in the adult brain,[3,4] another line of evidence has demonstrated that circulating monocytes can give rise to cerebral macrophages under inflammatory or pathologic conditions.[5–7] Our group has shown that bone marrow (BM)-derived cells infiltrate the damaged brain regions in the acute phase of a hypoxic-ischemic (HI) brain injury in mice. Most of the differentiated BM-derived cells acquired an activated macrophage phenotype,[6] further supporting the potential role of circulating monocytes in the pathophysiology of stroke.[8] These studies indicated that monocytes consist of a heterogeneous cell population that might represent potential targets for immunomodulatory therapies[9] as well as for the development of novel prognostic markers after stroke.[10,11]

Murine monocytes can be classified into two subpopulations: inflammatory (Ly6C^{hi}CX3CR1^{int}CCR2^{+}) and patrolling (Ly6C^{low} CX3CR1^{hi}CCR2^{-}) monocytes. These two subsets of monocytes have distinct sets of chemokine receptors and adhesion molecules, reflecting their respective functions and migratory properties.[12] Typically, inflammatory monocytes exit the bone marrow or the spleen to reach the bloodstream and infiltrate inflamed tissues in a CCR2-dependent fashion. Ultimately, they differentiate into macrophages and dendritic cells.[13] On the other side, while tissue extravasation of patrolling monocytes is possible,[14,15] the main fate of this subset of monocytes seem to be terminally differentiated blood-resident macrophages that act as intravascular 'housekeepers'.[16,17]

Recently, Gliem and colleagues reported the role of inflammatory monocytes in the maintenance of the integrity of the neurovascular unit after a stroke in mice. The study showed that bone marrow-derived cells recruited via CCR2 prevent the hemorrhagic transformation of stroke and delayed clinical deterioration.[18] However, the role of patrolling Ly6C^{low} monocytes after stroke is still unknown.

In this study, we generated bone marrow chimeric mice, in which the hematopoietic system was depleted and substituted by wild-type (WT) cells or by cells lacking the expression of the orphan nuclear receptor NR4A1 (also known as NUR77), a transcription factor that controls the differentiation and the survival of Ly6C^{low} monocytes.[19] Thereafter, we subjected these chimeric mice to cerebral HI, a rodent model of stroke,[20] to investigate the potential role of Ly6C^{low} monocytes in the progression of the injury.

Neuroscience Laboratory, CHU de Québec Research Center, Department of Molecular Medicine, Faculty of Medicine, Laval University, Québec City, Québec, Canada. Correspondence: Dr S Rivest, Neuroscience Laboratory, CHU de Québec Research Center, Department of Molecular Medicine, Faculty of Medicine, Laval University, 2705 Laurier Boulevard, Québec City, Québec, Canada G1V 4G2.
E-mail: Serge.Rivest@crchuq.ulaval.ca
This work was supported by the Canadian Institutes of Health Research, the Canadian Stroke Network, and the Canadian Stroke Network and European Stroke Network Collaborative Research Initiative. Jean-Philippe Michaud is supported by a doctoral scholarship from the Canadian Institutes of Health Research. *Nr4a1*$^{-/-}$ mice were generously provided by Dr Claude Rouillard (Laval University).
[2]These authors contributed equally to this work.
Received 24 January 2014; revised 26 March 2014; accepted 8 April 2014

Our results suggested that, despite having no functional Ly6C^{low} blood monocytes, chimeric mice lacking *Nr4a1* expression in their hematopoietic system displayed no major alterations in the structural and functional outcomes after stroke.

MATERIALS AND METHODS

Animals

Adult WT male mice were purchased from Charles River Laboratories whereas *Nr4a1*$^{-/-}$ mice were generously provided by Dr Claude Rouillard (Laval University, Québec, CA, USA). All mice had a pure C57BL/6J background and were acclimated to standard laboratory conditions (12-h light/dark cycle, lights on from 0715 to 1915 hours) with *ad libitum* access to mouse chow and water. All animal procedures were conducted according to the Canadian Council on Animal Care guidelines, as administered by the Laval University Animal Welfare Committee.

Generation of Chimeric Mice

Bone marrow cells were obtained by flushing femurs from WT or *Nr4a1*$^{-/-}$ donor mice (3 months of age) in a sterile environment. Cells were harvested using DPBS (Dulbecco's phosphate-buffered saline (Wisent, St-Jean-Baptiste de Rouville, QC, Canada) complemented with 2% fetal bovine serum. To remove clumps from the extract, the preparation was filtered using a 40-μm nylon filter and pelleted. The supernatant was removed and cells re-suspended in DPBS before being chased through a 25-g syringe needle. Cells were centrifuged and re-suspended in fresh DPBS. Three-month-old receiving WT mice were exposed to 10-gray total-body irradiation using a cobalt-60 source (Theratron-780; MDS Analytical Technologies, Concord, ON, Canada). Twenty-four hours later, the animals were administered freshly collected 1.5×10^7 BM cells via the tail vein (200 μL). Irradiated WT mice transplanted with WT BM cells (WT → WT) and irradiated WT mice transplanted with *Nr4a1*$^{-/-}$ BM cells (*Nr4a1*$^{-/-}$ → WT) were housed in sterile cages and treated with antibiotics (0.2 mg/mL trimethoprim and 1 mg/mL sulfamethoxazole; GlaxoSmithKline, Philadelphia, PA, USA) in the drinking water for 7 days before and up to 2 weeks after irradiation. The BM reconstitution procedure was confirmed 10 weeks later by flow cytometry analysis of blood leukocytes.

Hypoxic-Ischemic Injury and Sham Surgery

Six-month-old WT → WT, *Nr4a1*$^{-/-}$ → WT and WT mice were subjected to either sham surgery or to the permanent occlusion of the right common carotid artery followed by hypoxia. The HI injury was based on the Levine/Vannucci model as described by Adhami *et al.*[20] Briefly, a midline cervical incision was made and the right common carotid artery was exposed and double-ligated with 6-0 silk suture thread, under isoflurane anesthesia (2%). The sham surgery consisted of a midline cervical incision followed by the exposition of the right common carotid artery, under isoflurane anesthesia (2%). In both groups, the skin incision was closed with interrupted 6-0 silk sutures and the animals were then placed on a temperature-controlled blanket until they recovered from anesthesia. On average, the surgical procedure took 15 to 20 minutes for each animal. Two hours after the surgery, chimeric mice were exposed to hypoxia (8% O_2 balanced with 92% N_2) for 30 or 37 minutes. Non-chimeric mice were exposed to 30 minutes of hypoxia. Body weights were measured just before the surgery and were carefully monitored afterwards. To allow mice to feed easily, wet food was added to the bottom of all cages for 3 days after the surgery. Behavioral tests were performed 1 and 6 days after the surgery. Chimeric mice exposed to 30 minutes hypoxia were killed 14 days later whereas chimeric mice subjected to 37 minutes hypoxia were killed 7 days after. Non-chimeric mice were killed 24 hours, 4 days, or 14 days after the surgery. The total number of chimeric mice used in each experiment is shown in Table 1.

Table 1. Mouse survival after HI in chimeric mice with *Nr4a1*$^{-/-}$ or WT hematopoietic system

Time of survival assessment	*WT → WT*	*Nr4a1*$^{-/-}$ *→ WT*
37 minutes HI		
Immediately after hypoxia	$n = 17/19$ (89%)	$n = 11/19$ (58%)
7 d.p.i.	$n = 16/17$ (94%)	$n = 9/11$ (82%)
30 minutes HI		
Immediately after hypoxia	$n = 5/6$ (83%)	$n = 5/6$ (83%)
14 d.p.i.	$n = 5/5$ (100%)	$n = 5/5$ (100%)
Sham		
7 d.p.i.	$n = 8/8$ (100%)	$n = 11/11$ (100%)

d.p.i., day post injury; HI, hypoxia-ischemia; WT, wild type. Six-month-old *Nr4a1*$^{-/-}$ → WT and WT → WT mice were subjected to a sham surgery or to HI injury for 37 or 30 minutes. Mouse survival was assessed immediately after hypoxia and up to 7 d.p.i. or 14 d.p.i. (Results are expressed as: live mice/total mice (survival %).

Behavior Tests

The behavioral experimenter was blind to surgery and mouse genotype. Moreover, the order of examined mice was distributed randomly for each test. Neurologic function and sensorimotor performance were assessed with a slightly modified Garcia's scale:[21] spontaneous activity, symmetry in the movement of four limbs, forepaw outstretching, climbing and body proprioception (3 points each, maximum score of 15). In parallel, motor functions were evaluated with the rotarod and the body swing tests. For the rotarod test, mice were placed on the rotarod apparatus that accelerated at a 0.3 r.p.m./second pace and the average latency to fall from three trials (spaced by 5 minutes) was compiled. The body swing test was performed as previously described.[22] Briefly, mice were held by the tail at 3 cm above the ground. A swing was recorded each time the animal moved his head at more than 10 degrees from the vertical axis. The mouse had to return to its neutral position (0 degree relative to the vertical axis) before another swing was counted and 1 minute of rest was given every five swings. A total of 20 swings were compiled and the percentage of left-biased swings was calculated. Hippocampal-dependent spatial learning and memory was measured in the T-water maze test. The T-maze apparatus (length of stem 64 cm, length of arms 30 cm, width 12 cm, height of walls 16 cm) was made of clear fiberglass and filled with water (23 ± 1 °C) at a height of 12 cm. An escape platform (11×11 cm) was placed at the end of the target arm and was submerged 0.5 cm below the surface. The position of the platform was chosen randomly for each animal before testing. To evaluate left–right spatial learning, the mice were placed in the stem of the T-maze and swam freely until they found the submerged platform (located either in the right or in the left arm of the T-maze apparatus) and escaped to it. If the animals did not find the platform within 60 seconds, they were gently guided onto it. After reaching the platform, the mice remained on it for 20 seconds. During the learning paradigm, the escape latency (time to reach the platform) was recorded for each trial, for a total of eight trials.

Flow Cytometry Analysis on Mouse Whole Blood

Blood (100 μL) was taken from the facial vein and kept in ethylenediaminetetraacetic acid coated vials (Sarstedt, Montréal, QC, Canada). Within 30 minutes, blood was pipetted into polystyrene tubes (BD Bioscience, Mississauga, ON, Canada) and incubated on ice with rat anti-mouse CD16/CD32 antibodies (clone 2.4G2; BD Biosciences) for 20 minutes. Cells were stained for 40 minutes with the following antibodies at their predetermined optimal concentration: V500-conjugated rat anti-mouse CD45 (clone 30-F11; BD Biosciences), A700-conjugated rat anti-mouse CD11b (clone M1/70; eBioscience, San Diego, CA, USA), APC-conjugated rat anti-mouse CD115 (clone AFS98; eBioscience), V450-conjugated rat anti-mouse Ly6C (AL-21; BD Biosciences), and PE-conjugated rat anti-mouse Ly6G (clone 1A8; BD Biosciences). Red blood cells were lysed with BD Pharm Lyse (BD Biosciences) according to the manufacturer's instructions. Samples were washed with DPBS and acquired on a flow cytometer (BD LSR II, Mississauga, ON, Canada) and data was analyzed with the FlowJo software v10 (Tree Star; Ashland, OR, USA). Cell debris and doublets were excluded from the analysis.

Tissue Collection

Brain collection and immunofluorescence were performed as previously described.[23] Briefly, mice were deeply anesthetized via an intraperitoneal injection of a mixture of ketamine (100 mg/mL)/xylazine (1 mg/mL) (Vetalar, Bioniche, Belleville, ON/Rompun, Bayer, Toronto, ON, Canada)

and then perfused intracardially with ice-cold 0.9% saline. Brains were rapidly removed from the skulls and postfixed for 3 days in 4% paraformaldehyde pH 7.4 at 4 °C, and then placed in a 4% paraformaldehyde solution containing 20% sucrose overnight at 4 °C. The frozen brains were mounted on a microtome (Leica Microsystems, Montréal, QC, Canada) and cut into 25-μm coronal sections. The slices were collected in cold cryoprotectant solution (0.05 M sodium phosphate buffer, pH 7.3, 30% ethylene glycol, and 20% glycerol) and stored at −20 °C.

Immunohistochemistry and Immunofluorescence

Free-floating sections were washed with KPBS (potassium phosphate-buffered saline; 3 × 10 minutes) and then incubated for 30 minutes in a permeabilization/blocking solution containing 4% goat serum, 1% bovine serum albumin, and 0.4% Triton X-100 (Sigma-Aldrich, Oakville, ON, Canada) in KPBS. Sections were incubated overnight with the rabbit anti-mouse Iba1 primary antibody (Wako Chemicals, Richmond, VA, USA) diluted in the same permeabilization/blocking solution, at 4°C. The sections were then rinsed in KPBS (3 × 10 minutes), followed by 90-minute incubation with a biotinylated goat anti-rabbit IgG (H + L) secondary antibody (Vector Laboratories, Burlington, ON, Canada). Sections were rinsed again in KPBS (3 × 10 minutes). Binding was visualized using the peroxidase-based Vectastain ABC kit (Vector Laboratories) and 3,3′-diaminobenzidine. Tissues were thereafter stained (Nissl staining) with thionin (0.25%), dehydrated through graded concentrations of alcohol, cleared in xylene, and coverslipped with DPX mounting media (Electron Microscopy Sciences, QC, Canada). Bright field images were taken using a Nikon C80i microscope equipped with both a motorized stage (Ludl, Hawthorne, NY, USA) and a Microfire charge couple device (CCD) color camera (Optronics, Baltimore, MD, USA). Cell quantification and brain damage were measured as previously described.[24] Cells counts and areas were performed by a masked experimenter on three brain sections (bregma −1.58, −1.82, and −2.18 mm) per animal with the Stereo Investigator software. Briefly, the following contours were traced for each hemisphere as virtual overlay on the real-time images obtained: total hemisphere, total infarct, hippocampus, hippocampus infarct, and hippocampal regions CA1/CA2, CA3, and DG. Iba1$^+$ cells in the hippocampus were quantified in the same sections and cell density was calculated by reporting the number of cells on the hippocampus area. CD68 and Iba1 immunofluorescence was performed as previously described[24] and the percentage of CD68$^+$ area covered was quantified with ImageJ using the same pixel intensity threshold for all pictures.

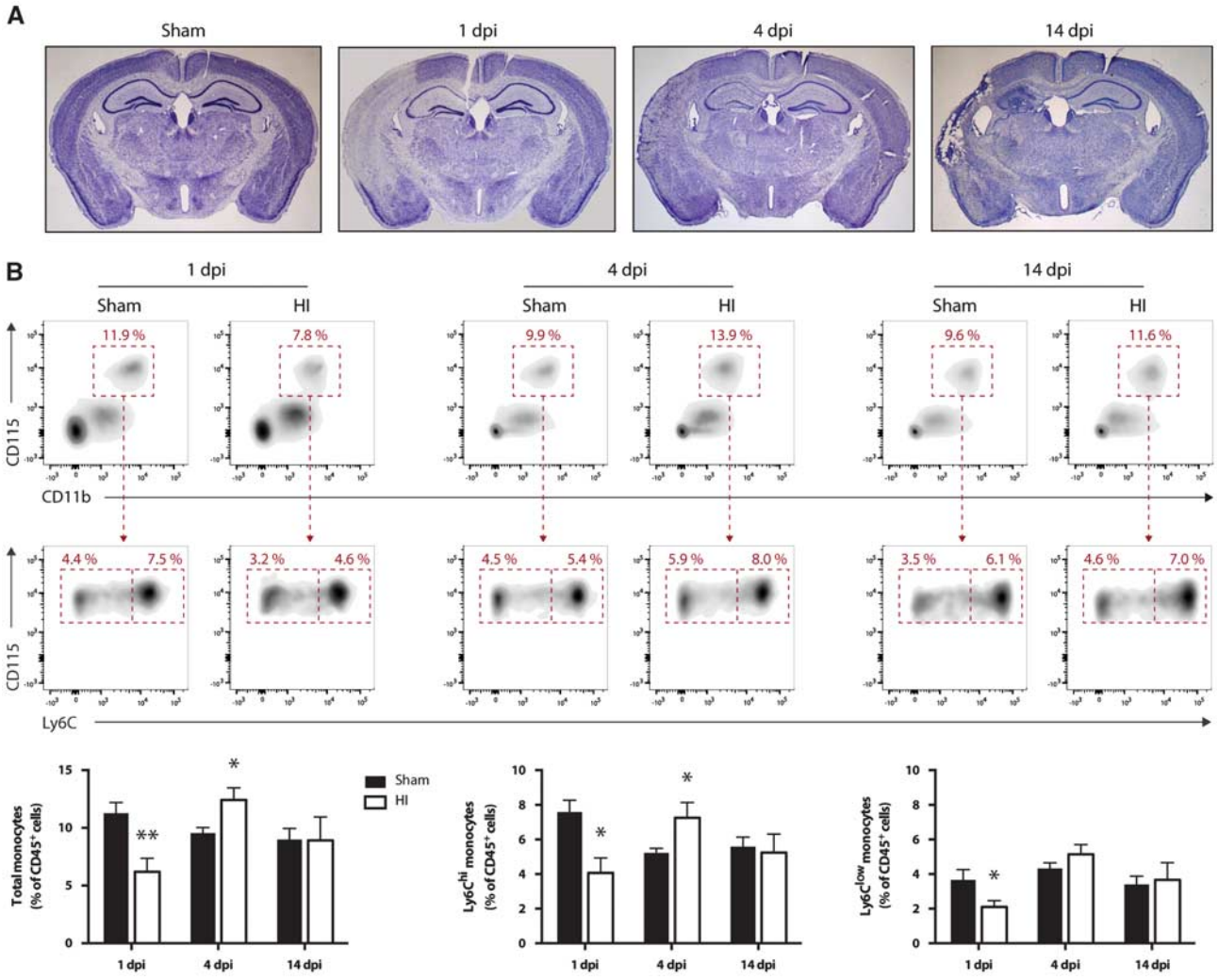

Figure 1. Hypoxic-ischemic-induced brain infarction and modulation of blood monocytes levels. Hypoxia-ischemia (HI) was induced in 6-month-old male mice by the permanent occlusion of the right common carotid artery followed by exposure to hypoxia (8% O_2, 92% N_2) for 30 minutes. (**A**) Representative photomicrographs of Nissl-stained coronal brain sections at different time points after HI. There is marked neuronal loss starting at 1 day post injury (d.p.i.) and a progressive cerebral atrophy of the ipsilateral hemisphere (left) compared with the noninjured contralateral side (right). (**B**) Flow cytometric analysis of blood monocytes after HI. Monocytes were identified by the expression of the following surface antigens: CD45$^+$CD11b$^+$CD115$^+$Ly6G$^-$ whereas Ly6C^{hi} monocytes and Ly6C^{low} monocytes subsets were separated based on their respective expression level of Ly6C (high versus low). (Results are expressed as means ± s.e.m.; $n = 5$ to 7. $^*P < 0.05$, $^{**}P < 0.01$ (versus sham); multiple Student's *t*-test).

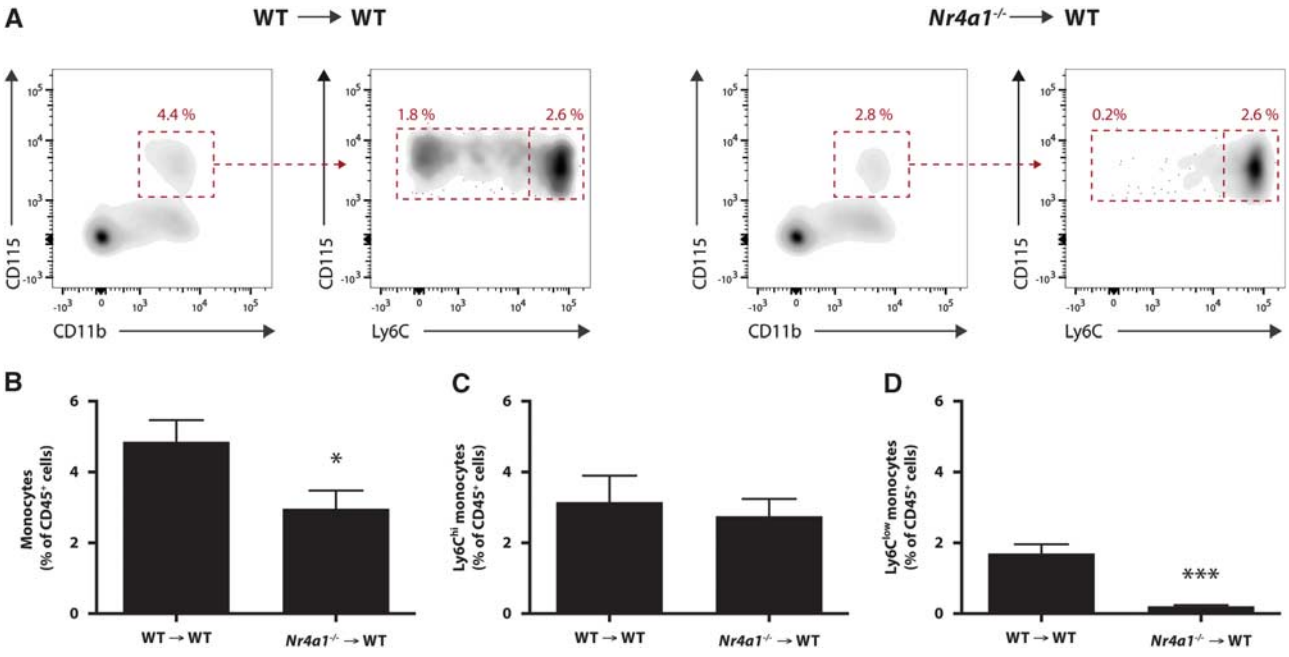

Figure 2. Chimeric wild-type (WT) mice with *Nr4a1*$^{-/-}$ hematopoietic system exhibit a selective loss of Ly6C^{low} monocytes. Three-month-old WT mice were lethally irradiated and transplanted with WT or *Nr4a1*$^{-/-}$ bone marrow cells. (**A**) Flow cytometric analysis of their blood monocytes was conducted 10 weeks later. (**B**) A slight decrease in total monocytes was observed in *Nr4a1*$^{-/-}$ → WT mice compared with WT → WT controls. (**C**) Ly6C^{hi} monocytes remained essentially unchanged between the two groups of chimeric mice. (**D**) Conversely, there was an important and significant diminution of Ly6C^{low} monocytes in *Nr4a1*$^{-/-}$ → WT mice compared with WT → WT mice. (Results are expressed as means ± s.e.m.; $n = 3$ to 5; *$P < 0.05$, ***$P < 0.001$; Student's *t*-test).

Statistical Analysis

All quantitative analysis were performed blind to the experimental conditions. Statistical analysis of the data was carried out with GraphPad Prism software (6.0a). The parametric Student's *t*-test, one-way analysis of variance and two-way analysis of variance were used. For non-parametric analysis, the Krustal–Wallis and Mann–Whitney *U*-test were applied. The level of significance was set at 0.05.

RESULTS

To characterize monocyte expansion in the bloodstream after a stroke in mice, we permanently occluded the right common carotid artery and exposed the mice to a hypoxic environment, as previously described.[20] As expected, this procedure leads to progressive changes in tissue structure, evident cell loss, and brain atrophy (Figure 1A). One day post injury (1 d.p.i.), flow cytometric analysis of blood monocytes revealed a significant reduction of total monocytes (Figure 1B). Thereafter, at 4 d.p.i., there was a significant increase of Ly6C^{hi} monocytes but the Ly6C^{low} subset remained unchanged (Figure 1B). At 14 d.p.i., all monocyte levels were at baseline values (Figure 1B).

To evaluate the role of Ly6C^{low} monocytes after a stroke, we generated chimeric mice to selectively and permanently deplete this circulating subset of monocytes without affecting resident microglia. As previously mentioned, the expression of the transcription factor NR4A1 in bone marrow hematopoietic cells is essential for the generation of functional Ly6C^{low} monocytes.[19] Therefore, 3-month-old WT recipient mice were lethally irradiated and transplanted with BM cells from either WT (from now on mentioned as WT → WT mice) or *Nr4a1*$^{-/-}$ mice (*Nr4a1*$^{-/-}$ → WT chimeras). Ten weeks later, blood monocytes were quantified by flow cytometry (Figure 2A). Although the amount of Ly6C^{hi} monocytes (Figure 2C) were not statistically different between the two groups, there was an important reduction of the amount of Ly6C^{low} monocytes in the blood of *Nr4a1*$^{-/-}$ → WT chimeras compared with WT → WT controls (Figure 2D). Consequently, this reduction of Ly6C^{low} monocytes led to a significant decrease of total monocytes (Figure 2B).

At 6 months of age, these chimeric mice were subjected to either sham surgery or HI brain injury. No mouse died 7 days after sham surgeries in the two groups (Table 1). However, two WT → WT and eight *Nr4a1*$^{-/-}$ → WT chimeras died during the 37-minute hypoxic insult, revealing a survival rate of 89% and 58%, respectively ($P = 0.06$; Fisher's exact test). Within the following 7 days, one WT → WT and two *Nr4a1*$^{-/-}$ → WT mice died. Considering the considerably low (58%) survival rate of *Nr4a1*$^{-/-}$ → WT chimeric mice after 37 minutes of hypoxia, we exposed additional mice to a shorter hypoxic episode of 30 minutes and monitored them for 14 days. In this case, only one chimera of each group died during the 30 minutes of hypoxia whereas all the others survived 14 d.p.i.

To compare the functional outcome between surviving WT → WT and *Nr4a1*$^{-/-}$ → WT mice after stroke, we monitored body weights and used complementary behavioral tests at 1 and 6 d.p.i. In both groups of chimeric mice, we observed significant lower body weights between the mice subjected to 37 minutes HI and the sham-operated group (Figure 3A). In mice exposed to 30 minutes HI, only *Nr4a1*$^{-/-}$ → WT mice had a significant loss of body weight compared with the sham group. *Post hoc* analysis revealed no difference between HI-injured mice with WT or *Nr4a1*$^{-/-}$ bone marrow cells. Although there was a general effect of the HI surgery (in both 37 and 30 minutes HI groups) in the neurologic score (Figure 3C) and in the rotarod test (Figure 3E), no *post hoc* difference was found between WT → WT and *Nr4a1*$^{-/-}$ → WT mice. At 6 d.p.i., there was no difference in body weights among the different groups (Figure 3B). Furthermore, most of the HI-injured mice seemed to have considerably recovered on the basis of their neurologic score (Figure 3D) and

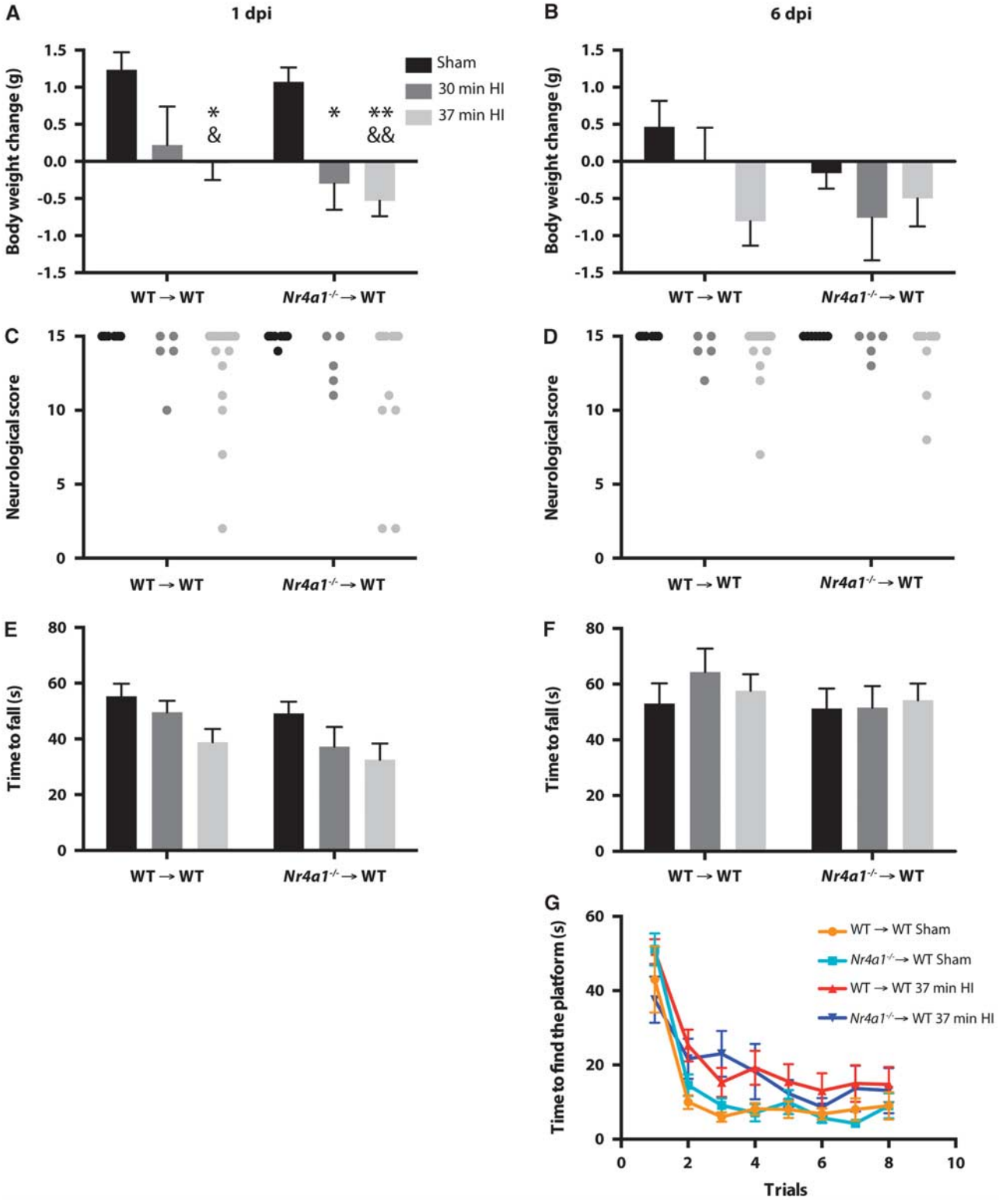

Figure 3. Physiologic and behavioral outcomes after HI in chimeric mice with *Nr4a1*$^{-/-}$ or WT hematopoietic system. *Nr4a1*$^{-/-}$ → WT and WT → WT mice had a sham surgery or were subjected to HI (right common carotid occlusion followed by 30 or 37 minutes of hypoxia). Changes in body weights were measured (**A**) 1 day or (**B**) 6 days after the surgery. To assess motor impairments post surgery, mice were evaluated with a neurologic test at (**C**) day 1 and (**D**) day 6, and a rotarod test at (**E**) day 1 and (**F**) day 6. (**G**) Hippocampal-dependent spatial learning was evaluated by the latency to find the localization of the platform in the water T-maze test 6 days after the surgery. Significant effects of the HI injuries were detected for **A**, **C**, **E,** and **G** (trials 2 and 3 only). (Results are expressed as means ± s.e.m.; each point represents a single mouse in **C** and **D**; *n* = all the mice alive in Table 1; for two-way analysis of variance (**A**, **B**, **E**, **F**, **G**), the Tukey *post hoc* test was performed; Kruskal–Wallis test was used in **C** and **D**; $^{*}P<0.05$, $^{**}P<0.01$ (versus WT → WT sham); $^{\&}P<0.05$, $^{\&\&}P<0.01$ (versus *Nr4a1*$^{-/-}$ → WT sham)). HI, hypoxia-ischemia; WT, wild type.

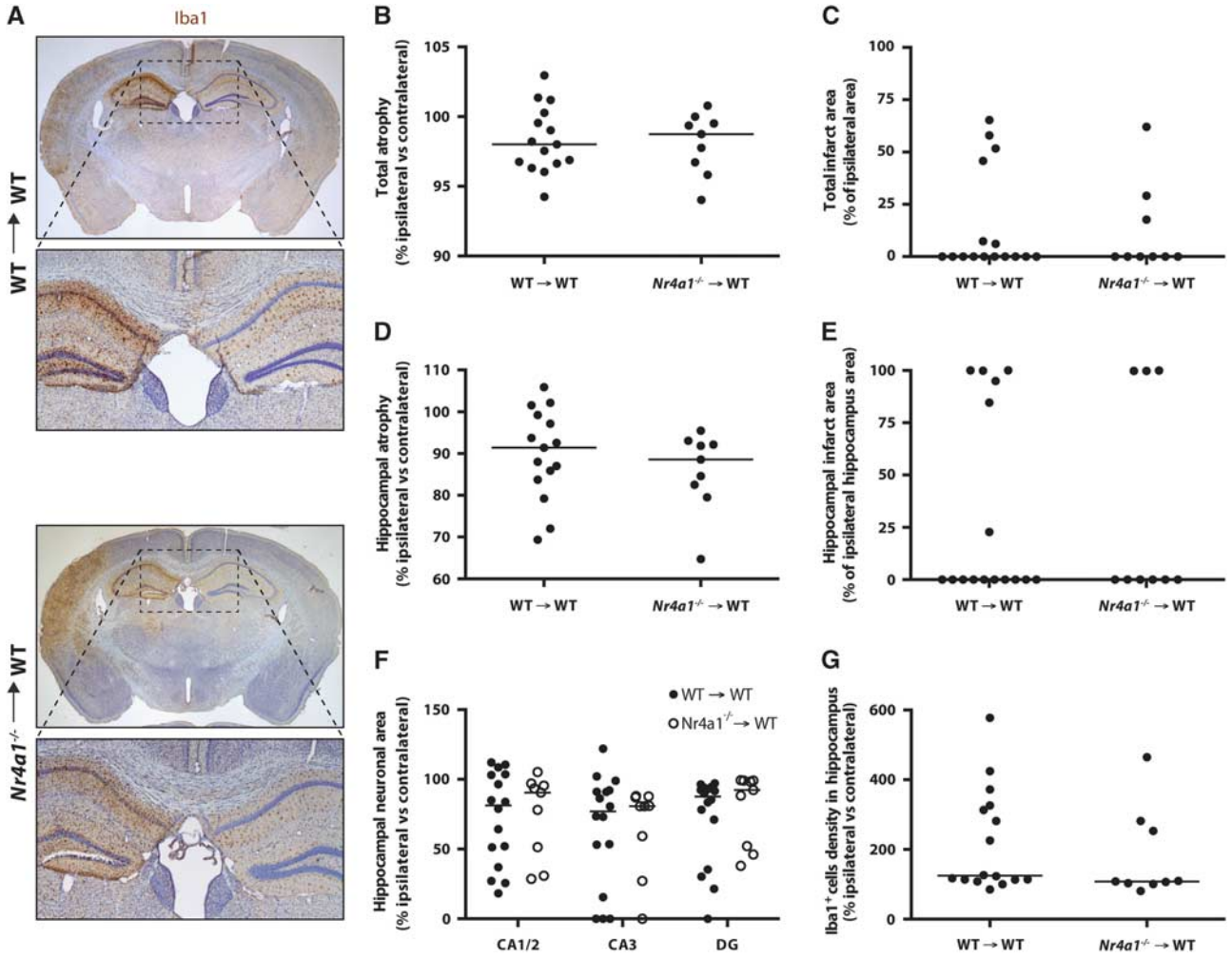

Figure 4. Brain damage and microgliosis in chimeric mice with *Nr4a1*$^{-/-}$ or WT hematopoietic system 7 days after 37 minutes HI. *Nr4a1*$^{-/-}$ → WT and WT → WT mice were subjected to sham surgery or to HI (right common carotid occlusion followed by 37 minutes of hypoxia) and were killed 7 days later. (**A**) Representative photomicrographs of Iba1- and Nissl-stained coronal brain sections of both groups. The following quantifications were performed on Nissl-stained coronal brain sections: (**B**) cerebral hemisphere atrophy, (**C**) total brain infarct area, (**D**) hippocampal atrophy, (**E**) hippocampal infarct area, and (**F**) hippocampal pyramidal neuronal area. These quantifications did not reveal any significant difference between the two experimental groups. (**G**) Quantification of microglia in coronal brain sections stained with the Iba1 antibody did not reveal any statistical difference in hippocampal microgliosis between the two groups of mice. DG, dentate gyrus. (each point represents a single mouse and the horizontal bars are the median for each group; $n = 9$ to 16; Mann–Whitney test). HI, hypoxia-ischemia; WT, wild type.

the time spent on the rotarod (Figure 3F). Considering that the HI mice did not show significant gross motor function impairments at 6 d.p.i., we assessed their spatial learning ability in the water T-maze test. Although we observed a significant effect of the stroke surgery in the second and third trials of the test, no statistical difference could be found between WT → WT and *Nr4a1*$^{-/-}$ → WT mice (Figure 3G).

We then quantified brain damage and microgliosis in WT → WT and *Nr4a1*$^{-/-}$ → WT mice, 7 days post 37 minutes HI injury. In addition to the total hemispheric lesion, we focused our quantification in the hippocampus, which is a very vulnerable brain region in this model of stroke (Figure 4A). Although there was evident structural damage after HI, no difference was observed between the two groups of chimeric mice for all the parameters examined; that is, the total brain atrophy (Figure 4B), total infarct area (Figure 4C), hippocampal atrophy (Figure 4D), hippocampal infarct area (Figure 4E), hippocampal neuronal loss in CA1/2, CA3, or dentate gyrus (Figure 4F), as well as for the number of microglia/macrophages in the damaged hippocampus (Figure 4G). Furthermore, no difference in CD68^{+} immunoreactivity was detected between the two groups (Figure 5), suggesting similar activation of microglia/macrophages. Finally, we performed the same measurements for mice subjected to 30 minutes HI and killed 14 days later. Again, no difference could be detected between the two groups of chimeric mice for all the parameters quantified (Supplementary Figure S1).

DISCUSSION

Hypoxic-ischemic events are followed by an inflammatory response involving leukocytes, the vascular system, and glial cells. Among leukocytes, monocytes are thought to patrol cerebral blood vessels and to infiltrate the brain parenchyma under pathologic conditions.[25,26] Although the time-course of blood monocyte subtypes has been characterized in patients after acute stroke,[10,27] similar data are not available in preclinical studies. In the present study, we observed a significant reduction of all types of blood monocytes in the first day after a HI brain injury in mice.

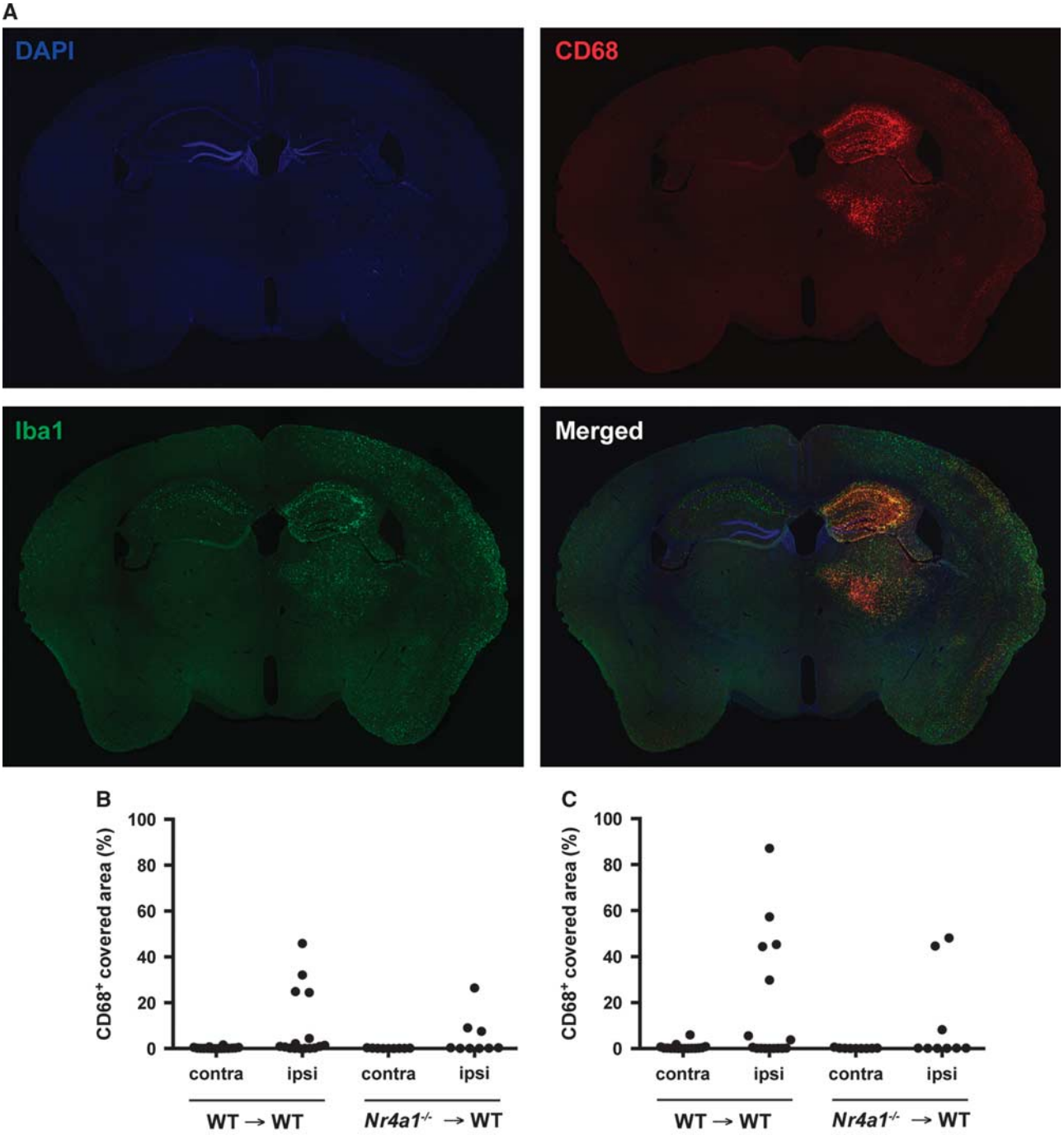

Figure 5. Similar CD68 immunoreactivity in the brain of chimeric mice with *Nr4a1*$^{-/-}$ or WT hematopoietic system 7 days after 37 minutes of HI. *Nr4a1*$^{-/-}$ → WT and WT → WT mice were subjected to sham surgery or to HI (right common carotid occlusion followed by 37 minutes of hypoxia) and were killed 7 days later. (**A**) Representative photomicrographs of DAPI, Iba1, and CD68 immunofluorescence. The quantification of CD68^{+} area covered in (**B**) the whole hemisphere or only in (**C**) the hippocampus did not reveal any statistical difference. (each point represents a single mouse; $n = 9$ to 16; Mann–Whitney test).

At 4 d.p.i., a significant increase of Ly6C^{hi} monocytes was measured in the blood, but not of the Ly6C^{low} subset. The timing of these changes is in accordance with a previous study showing that the number of circulating monocytes increases from 2 to 7 days after the injury in patients with stroke.[11] It also coincides with the recruitment of blood-derived macrophages/microglia to the ischemic brain, which is already observed at low levels in the first d.p.i., peaking at 3 to 5 days after the insult.[6,18,28,29] In this scenario, future studies will be necessary to identify whether the changes in monocyte levels in the first days after HI are caused by an imbalance between monocytopoiesis (and/or monocyte release into the blood) and brain infiltration from the bloodstream. In this regard, it is known that myeloid cells from the bone marrow rapidly respond to experimental stroke[30] and that splenic monocytopoiesis can occur in mice subjected to middle cerebral artery occlusion.[31] It is possible that monocyte recruitment surpasses their production or release into the blood in the first d.p.i., whereas the opposite phenomenon occurs in the

following days. Eventually, we also observed that blood monocyte levels returned to baseline values at 14 d.p.i., which is compatible with the current view that monocyte infiltration occurs mainly within the first few days after stroke induction.[6,18,29]

Although monocytes (and more specifically inflammatory CCR2^{+} monocytes) seem crucial to prevent hemorrhagic transformation and clinical deterioration after stroke,[18] the specific role of patrolling monocytes remains unanswered. Gliem *et al*[18] relied on three strategies for monocytes depletion: clodronate-encapsulated liposomes, CD11b-DTR mice and CCR2$^{-/-}$ BM chimeric mice. These approaches undoubtedly affect the Ly6C^{low} subset because Ly6C^{hi} inflammatory monocytes are obligatory precursors of Ly6C^{low} monocytes.[17] Interestingly, in *Nr4a1*$^{-/-}$ mice, Ly6C^{low} are eliminated whereas Ly6C^{hi} levels are not affected. Importantly, mice with *Nr4a1*$^{-/-}$ hematopoietic system generate the same number of dendritic cells, natural killer T cells, B cells, and T cells, while only slightly increasing (<10%) granulocytes concentration.[19] In the present study, we generated *Nr4a1*$^{-/-}$ → WT chimeric mice to permanently and selectively deplete Ly6C^{low} monocytes and evaluate the role of these cells after cerebral HI. This approach allowed us to assess the effect of knocking out *Nr4a1* expression specifically in cells of the hematopoietic system. This is a crucial aspect of this study because *Nr4a1* is an immediate early gene whose expression in neurons is upregulated after excitotoxic insults *in vitro*[32] and after cerebral ischemia *in vivo*.[33] *Nr4a1* knockdown also increases cell death of cerebellar neurons subjected to oxygen and glucose deprivation.[34] In addition, *Nr4a1* has been reported to regulate other cell functions such as metabolism, energy homeostasis, apoptosis, proliferation, and inflammation.[35]

Our first finding indicated that Ly6C^{low} monocytes seemed to contribute to the survival of adult mice during a hypoxic event of 37 minutes. However, no significant statistical difference could be detected. Nonetheless, the surviving *Nr4a1*$^{-/-}$ → WT chimeric mice had a similar infarct volume in the ipsilateral hemisphere and in the hippocampus, compared with WT → WT controls. In addition, no difference between the groups was observed when the neurologic function was examined for up to 6 days after the injury. Given the different rate of survival between the two groups after 37 minutes of hypoxia, we subjected another batch of animals to 30 minutes of hypoxia, as a way to overcome the potential bias of evaluating only the animals that survived. With this protocol, we obtained a decreased mortality rate, which was similar for both groups. Nevertheless, both groups exhibited a similar pattern of brain damage and neurologic deficits after the HI insult. The interpretation of the data of this 30-minute HI protocol is limited because of the number of animals used. However, no major difference was observed between the two groups of mice, which does not support the possibility that a significant bias could have been introduced by higher mortality in *Nr4a1*$^{-/-}$ → WT chimeric mice after 37 minutes of HI.

Overall, these observations indicate that, despite the effective absence of Ly6C^{low} monocytes in *Nr4a1*$^{-/-}$ → WT chimeric mice, there was no major change in the structural and functional outcomes usually utilized to evaluate the progression and the severity of experimental stroke. This is a surprising finding if we consider the role of Ly6C^{low} monocytes in other inflammatory conditions, such as in the clearance of vascular Amyloid beta in Alzheimer's disease,[36] tissue repair after myocardium infarct[14] and dampening atherosclerosis.[37] Although it is not affecting the progression of major outcomes after stroke; we cannot exclude the possibility that Ly6C^{low} monocytes could be involved in other functions that do not directly affect the investigated parameters, such as neural plasticity or vascular regeneration. Also, it is conceivable that the functions or the numbers of other recruited leukocytes, such as neutrophils, could be modulated in mice without Ly6C^{low} monocytes. In this study, the absence of Ly6C^{low} monocytes did not affect the number or the activation state of microglia/macrophages in the damaged regions. There is evidence that Ly6C^{low} monocytes can infiltrate the injured spinal cord,[38,39] but the fact that the number of Iba1^{+} cells remained unchanged in our study suggest that these monocytes contribute minimally or do not contribute to the microglia/macrophage pool in the HI brain parenchyma. This is in agreement with reports suggesting the differentiation of Ly6C^{hi} into Ly6C^{low} macrophages in stroke[18] and muscle regeneration.[40] Supporting this hypothesis, Gliem *et al*[18] have shown that the recruitment of macrophages to the ischemic brain is mainly dependent on CCR2, which is highly expressed by Ly6C^{hi} inflammatory monocytes but absent on Ly6C^{low} patrolling monocytes. This condition shares some similarities with the animal model of multiple sclerosis, in which there is also the breakdown of the blood–brain barrier and the infiltration of monocytes that occurs primarily via CCR2.[41]

In conclusion, our data suggest that Ly6C^{low} patrolling monocytes have a redundant role in the progression of structural damage and neurologic deficits after cerebral HI.

DISCLOSURE/CONFLICT OF INTEREST

The authors declare no conflict of interest.

ACKNOWLEDGMENTS

The authors thank Marc-André Bellavance, Nataly Laflamme, Marie-Michèle Plante and Nadia Fortin for technical assistance.

REFERENCES

1 Lozano R, Naghavi M, Foreman K, Lim S, Shibuya K, Aboyans V *et al.* Global and regional mortality from 235 causes of death for 20 age groups in 1990 and 2010: a systematic analysis for the Global Burden of Disease Study 2010. *Lancet* 2012; **380**: 2095–2128.
2 Iadecola C, Anrather J. The immunology of stroke: from mechanisms to translation. *Nat Med* 2011; **17**: 796–808.
3 Ginhoux F, Greter M, Leboeuf M, Nandi S, See P, Gokhan S *et al.* Fate mapping analysis reveals that adult microglia derive from primitive macrophages. *Science* 2010; **330**: 841–845.
4 Kierdorf K, Erny D, Goldmann T, Sander V, Schulz C, Perdiguero EG *et al.* Microglia emerge from erythromyeloid precursors via Pu.1- and Irf8-dependent pathways. *Nat Neurosci* 2013; **16**: 273–280.
5 London A, Cohen M, Schwartz M. Microglia and monocyte-derived macrophages: functionally distinct populations that act in concert in CNS plasticity and repair. *Front Cell Neurosci* 2013; **7**: 34.
6 Lampron A, Pimentel-Coelho PM, Rivest S. Migration of bone marrow-derived cells into the central nervous system in models of neurodegeneration. *J Comp Neurol* 2013; **521**: 3863–3876.
7 Ajami B, Bennett JL, Krieger C, McNagny KM, Rossi FMV. Infiltrating monocytes trigger EAE progression, but do not contribute to the resident microglia pool. *Nat Neurosci* 2011; **14**: 1142–1149.
8 Chamorro Á, Meisel A, Planas AM, Urra X, van de Beek D, Veltkamp R. The immunology of acute stroke. *Nat Rev Neurol* 2012; **8**: 401–410.
9 Shechter R, Schwartz M. Harnessing monocyte-derived macrophages to control central nervous system pathologies: no longer 'if' but 'how'. *J Pathol* 2013; **229**: 332–346.
10 Urra X, Villamor N, Amaro S, Gómez-Choco M, Obach V, Oleaga L *et al.* Monocyte subtypes predict clinical course and prognosis in human stroke. *J Cereb Blood Flow Metab* 2009; **29**: 994–1002.
11 Urra X, Cervera A, Obach V, Climent N, Planas AM, Chamorro Á. Monocytes are major players in the prognosis and risk of infection after acute stroke. *Stroke* 2009; **40**: 1262–1268.
12 Geissmann F, Auffray C, Palframan R, Wirrig C, Ciocca A, Campisi L *et al.* Blood monocytes: distinct subsets, how they relate to dendritic cells, and their possible roles in the regulation of T-cell responses. *Immunol Cell Biol* 2008; **86**: 398–408.
13 Serbina NV, Pamer EG. Monocyte emigration from bone marrow during bacterial infection requires signals mediated by chemokine receptor CCR2. *Nat Immunol* 2006; **7**: 311–317.
14 Nahrendorf M, Swirski FK, Aikawa E, Stangenberg L, Wurdinger T, Figueiredo J-L *et al.* The healing myocardium sequentially mobilizes two monocyte subsets with divergent and complementary functions. *J Exp Med* 2007; **204**: 3037–3047.

15 Auffray C, Fogg D, Garfa M, Elain G, Join-Lambert O, Kayal S *et al.* Monitoring of blood vessels and tissues by a population of monocytes with patrolling behavior. *Science* 2007; **317**: 666–670.
16 Carlin LM, Stamatiades EG, Auffray C, Hanna RN, Glover L, Vizcay-Barrena G *et al.* Nr4a1-dependent Ly6C(low) monocytes monitor endothelial cells and orchestrate their disposal. *Cell* 2013; **153**: 362–375.
17 Yona S, Kim K-W, Wolf Y, Mildner A, Varol D, Breker M *et al.* Fate mapping reveals origins and dynamics of monocytes and tissue macrophages under homeostasis. *Immunity* 2013; **38**: 79–91.
18 Gliem M, Mausberg AK, Lee J-I, Simiantonakis I, van Rooijen N, Hartung H-P *et al.* Macrophages prevent hemorrhagic infarct transformation in murine stroke models. *Ann Neurol* 2012; **71**: 743–752.
19 Hanna RN, Carlin LM, Hubbeling HG, Nackiewicz D, Green AM, Punt JA *et al.* The transcription factor NR4A1 (Nur77) controls bone marrow differentiation and the survival of Ly6C- monocytes. *Nat Immunol* 2011; **12**: 778–785.
20 Adhami F, Liao G, Morozov YM, Schloemer A, Schmithorst VJ, Lorenz JN *et al.* Cerebral ischemia-hypoxia induces intravascular coagulation and autophagy. *Am J Pathol* 2006; **169**: 566–583.
21 Garcia JH, Wagner S, Liu KF, Hu XJ. Neurological deficit and extent of neuronal necrosis attributable to middle cerebral artery occlusion in rats. Statistical validation. *Stroke* 1995; **26**: 627–634, discussion 635.
22 Borlongan CV, Sanberg PR. Elevated body swing test: a new behavioral parameter for rats with 6-hydroxydopamine-induced hemiparkinsonism. *J Neurosci* 1995; **15**: 5372–5378.
23 Simard AR, Soulet D, Gowing G, Julien J-P, Rivest S. Bone marrow-derived microglia play a critical role in restricting senile plaque formation in Alzheimer's disease. *Neuron* 2006; **49**: 489–502.
24 Pimentel-Coelho PM, Michaud J-P, Rivest S. Evidence for a gender-specific protective role of innate immune receptors in a model of perinatal brain injury. *J Neurosci* 2013; **33**: 11556–11572.
25 Courties G, Moskowitz MA, Nahrendorf M. The innate immune system after ischemic injury: lessons to be learned from the heart and brain. *JAMA Neurol* 2013; **71**: 233–236.
26 Prinz M, Priller J. Tickets to the brain: role of CCR2 and CX3CR1 in myeloid cell entry in the CNS. *J Neuroimmunol* 2010; **224**: 80–84.
27 Kaito M, Araya S-I, Gondo Y, Fujita M, Minato N, Nakanishi M *et al.* Relevance of distinct monocyte subsets to clinical course of ischemic stroke patients. *PLoS ONE* 2013; **8**: e69409.
28 Chu HX, Kim HA, Lee S, Moore JP, Chan CT, Vinh A *et al.* Immune cell infiltration in malignant middle cerebral artery infarction: comparison with transient cerebral ischemia. *J Cereb Blood Flow Metab* 2013; **34**: 450–459.
29 Li T, Pang S, Yu Y, Wu X, Guo J, Zhang S. Proliferation of parenchymal microglia is the main source of microgliosis after ischaemic stroke. *Brain* 2013; **136**: 3578–3588.
30 Denes A, McColl BW, Leow-Dyke SF, Chapman KZ, Humphreys NE, Grencis RK *et al.* Experimental stroke-induced changes in the bone marrow reveal complex regulation of leukocyte responses. *J Cereb Blood Flow Metab* 2011; **31**: 1036–1050.
31 Leuschner F, Rauch PJ, Ueno T, Gorbatov R, Marinelli B, Lee WW *et al.* Rapid monocyte kinetics in acute myocardial infarction are sustained by extramedullary monocytopoiesis. *J Exp Med* 2012; **209**: 123–137.
32 Jacobs CM, Boldingh KA, Slagsvold HH, Thoresen GH, Paulsen RE. ERK2 prohibits apoptosis-induced subcellular translocation of orphan nuclear receptor NGFI-B/TR3. *J Biol Chem* 2004; **279**: 50097–50101.
33 Küry P, Schroeter M, Jander S. Transcriptional response to circumscribed cortical brain ischemia: spatiotemporal patterns in ischemic vs. remote non-ischemic cortex. *Eur J Neurosci* 2004; **19**: 1708–1720.
34 Xiao G, Sun T, Songming C, Cao Y. NR4A1 enhances neural survival following oxygen and glucose deprivation: an in vitro study. *J Neurol Sci* 2013; **330**: 78–84.
35 Zhao Y, Bruemmer D. NR4A orphan nuclear receptors: transcriptional regulators of gene expression in metabolism and vascular biology. *Arterioscler Thromb Vasc Biol* 2010; **30**: 1535–1541.
36 Michaud J-P, Bellavance M-A, Préfontaine P, Rivest S. Real-time in vivo imaging reveals the ability of monocytes to clear vascular amyloid beta. *Cell Rep* 2013; **5**: 646–653.
37 Hanna RN, Shaked I, Hubbeling HG, Punt JA, Wu R, Herrley E *et al.* NR4A1 (Nur77) deletion polarizes macrophages toward an inflammatory phenotype and increases atherosclerosis. *Circ Res* 2012; **110**: 416–427.
38 Donnelly DJ, Longbrake EE, Shawler TM, Kigerl KA, Lai W, Tovar CA *et al.* Deficient CX3CR1 signaling promotes recovery after mouse spinal cord injury by limiting the recruitment and activation of Ly6Clo/iNOS+ macrophages. *J Neurosci* 2011; **31**: 9910–9922.
39 Shechter R, Miller O, Yovel G, Rosenzweig N, London A, Ruckh J *et al.* Recruitment of beneficial M2 macrophages to injured spinal cord is orchestrated by remote brain choroid plexus. *Immunity* 2013; **38**: 555–569.
40 Varga T, Mounier R, Gogolak P, Poliska S, Chazaud B, Nagy L. Tissue LyC6- macrophages are generated in the absence of circulating LyC6- monocytes and Nur77 in a model of muscle regeneration. *J Immunol* 2013; **191**: 5695–5701.
41 Mildner A, Mack M, Schmidt H, Brück W, Djukic M, Zabel MD *et al.* CCR2+Ly-6Chi monocytes are crucial for the effector phase of autoimmunity in the central nervous system. *Brain* 2009; **132**: 2487–2500.

Supplementary Information accompanies the paper on the Journal of Cerebral Blood Flow & Metabolism website (http://www.nature.com/jcbfm)